KINEMATICS AND MODELLING OF A SYSTEM FOR ROBOTIC SURGERY

Hermann Mayer, István Nagy and Alois Knoll
Robotics and Embedded Systems
Technische Universität München
{mayerh|nagy|knoll}@in.tum.de

Abstract We have developed an open experimental platform for robot assisted minimally invasive heart surgery with haptic feedback. The manipulator set-up is composed of two low-payload robots carrying delicate surgical instruments. One of the main requirements is full Cartesian control of the end effectors to enable the surgeon to precisely control the position and orientation of the instruments. This must be realized in the presence of severe mechanical constraints imposed by the small ports ("key holes") in the patient's body which drastically restrict the motion space of the instrument. In this paper we present the complete set-up with the underlying theory and the software simulator that allows us to test operations before applying them to the real system.

Keywords: robotic heart surgery, minimally invasive surgery, trocar kinematics

1. Introduction

Minimally invasive surgery (MIS) has become a promising option for a great number of medical interventions (like coronary heart surgery). However, apart from obvious advantages to the patient (including reduced tissue trauma and shorter recovery times), using this technique entails additional difficulties. The basic limitations are reduced sight and manipulability. This gap is closed by application of robotic systems. Available systems like the *daVinci* workstation (cf. G. Guthart and J. Salisbury, 2000) or the *ZEUS* system provide the surgeon with stereo vision of the operating environment and restore full control of the instruments. While having pioneered the field of endoscopic surgery, these systems suffer from several deficiencies: they are telemanipulators with no direct position control (the control loop is implicitly closed by visual servoing of the surgeon) and they provide no possibility for force feedback. Both features are important in order to move the surgeon up in the control hierarchy, i.e. to implement "partial autonomy". There is a number of research projects that aim at remedying these deficiencies. At the University of California, Berkeley, a robotic system was developed, which has already been used to perform certain surgi-

cal tasks like suturing and knot-tying (M. Cavusoglu et al., 2003). The Korean Advanced Institute of Science and Technology has developed a micro-telerobot system that also provides force feedback (D. Kwon et al., 1998). In Germany two systems for robotic surgery were built at the Research Facility in Karlsruhe (U. Voges et al. 1997) and at the DLR in Oberpfaffenhofen (R. Konietschke et al., 2003). While the first system provides no force feedback, the latter system is equipped with *PHANToM* devices for haptic display.

The goal of our prototypical system is three-fold: (i) implementing full Cartesian control of the combination of robot and articulated instrument along with software facilities for realistic simulation, (ii) meeting all the requirements for sensitive force feedback enabling complex and complicated surgical procedures like knot-tying, and (iii) providing an open experimental platform for researchers that have no access to proprietary software interfaces of the other systems. In the scope of this paper we will concentrate on (i) and describe the mechanical properties of our platform and sketch the simulator.

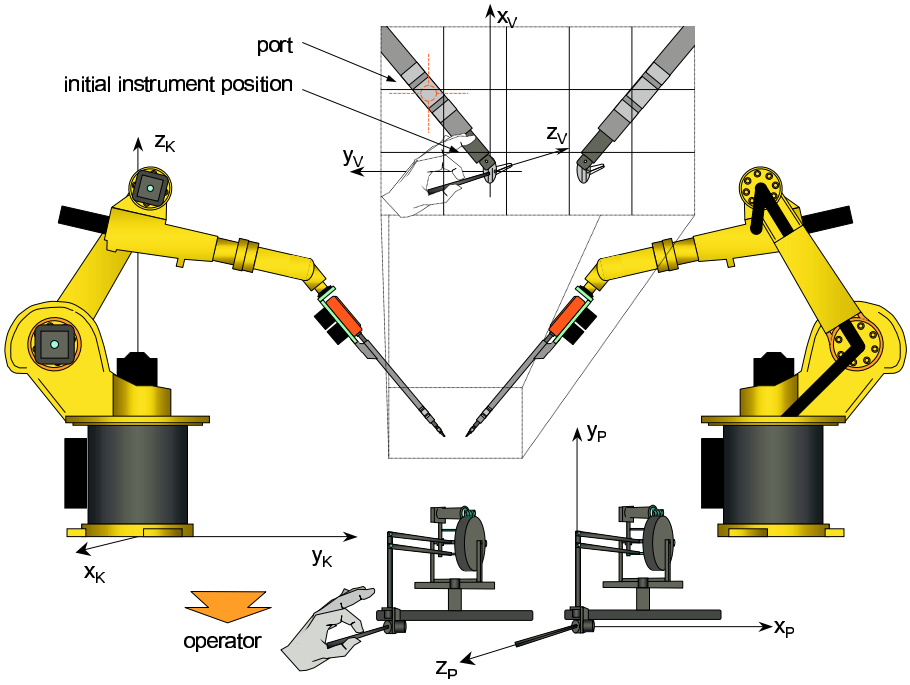

Figure 1. System Overview

2. System Setup and Virtual Instrument

The motor part of our system consists mainly of two instruments for minimally invasive surgery, which are mounted on industrial-grade low-payload robots (Fig. 1). To address the aspect of intuitive operability of the user interface, we apply the concept of so-called *trocar kinematics*: the manipulator has to pass through a fixed hole ("port") in the the patient's body. This restricts the degrees of freedom of the instrument. Feed (translation) and rotation axes must always intersect with the fixed port. Given the position and rotation of the end effector, we have to calculate all joint angles of our eight degrees of freedom (DOF) system. The resulting angles can be directly applied to the robotic system – or they can first be evaluated in a simulation environment.

Because the system's working space is mostly determined by the working space of the robots, we have chosen their base coordinate system K as our base system. In our setup, the surgeon (handling two haptic input devices of type *PHANToM*) and the observation camera, respectively, are placed in front of the robots: the x_K-axis points in the direction of the user, while the z_K-axis points upward to the ceiling (Fig. 1). The force-feedback styluses are placed in front of the user and, therefore, the z_P-axis is collinear with the x_K-axis of the robot system. The y_P-axis points up to the ceiling, while the x_P-axis points to the right hand side (Fig. 1).

The specification of the coordinate system for the minimally invasive instrument is crucial for all further considerations. As mentioned above, we want to make the control of the instrument appear to the surgeon as "natural" or "intuitive". We therefore modelled the kinematic structure on the observation of the human hand: if humans perform very precise manual tasks (e.g. a surgeon making a cut), we turn the hand about a rotation center that lies near the first link of the fingers (Fig. 2, left). If we want to mimic this behavior in our instrument control – while preserving mechanical feasibility – then a good compromise is a setting as shown in Fig. 2, center. We call the coordinate system spanned by the axes x_V, y_V and z_V the virtual instrument system. The mechanical rotation axes of the real instrument are named x_M, y_M and z_M (Fig. 2, right).

3. Trocar Kinematics

As mentioned above, all instruments have to pass through the incisions in the patient's body (ports). In most cases three ports are needed (see Fig. 3); two ports for the instruments and one port for the endoscopic stereo camera. Clearly, the possible movement of the instrument's shaft

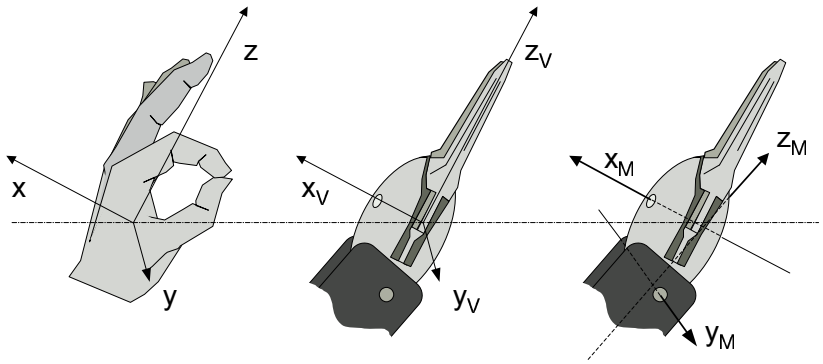

Figure 2. Virtual Instrument Definition

is restricted to insertion, retraction and rotation about the center axis of the corresponding port P.

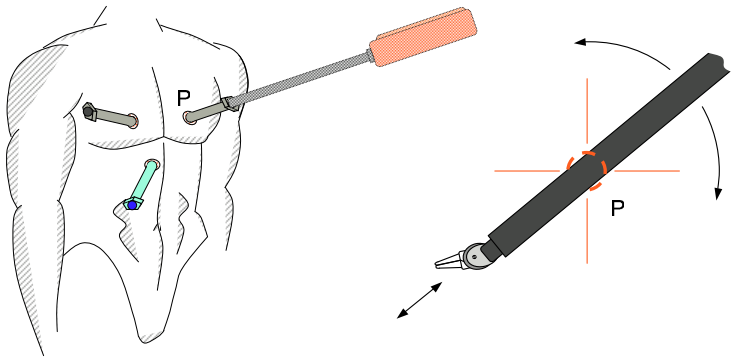

Figure 3. Location of the Instrument and Camera Port

The most comfortable way of moving a surgical instrument inside the body would be Cartesian control. The homogeneous transformation matrix ${}^{K}_{V}T$ describing the pose of the virtual instrument is given by the position of the input stylus of the *PHANToM* haptic devices.

We now determine the transformation matrix for an *initial* instrument system I. This system is the initial virtual instrument system V with all instrument angles set to zero. The basic idea is that we can easily calculate the homogenous transformation of this system in relation to the robot system. Then, the system I can be transferred to the virtual instrument system V by subsequent rotations of shaft, wrist and fingers.

First, we describe the rotation of system I, relative to the base (robot) system, by Z-Y-X-Euler angles:

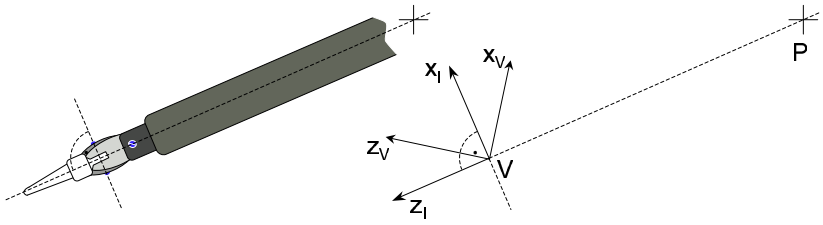

Figure 4. Initial Position of the Virtual Instrument

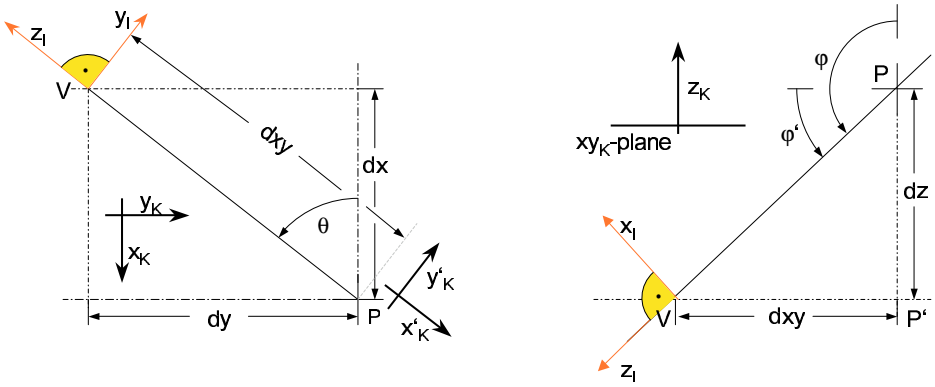

Figure 5. Z-Y-(X)-Euler Angles of the Virtual Instrument System

Because we know the position of the port P and the instrument V, we can derive the Z-Y-Euler angles θ and φ from the geometry shown in Fig. 5. Rotation about the x-axis is set to zero (therefore y_I is parallel to the xy_K plane. We have:

$$\theta = atan2(dy, dx) \quad (1)$$

$$\varphi = atan2(dz, dxy) + 90° \quad (2)$$

With these angles we can now arrange the homogenous rotation matrix ${}^K_I T$ that transforms the robot base system to the initial position of the instrument. The derivation of this relation is straightforward and well-known (e.g. J. Craig, 1986 or T. Yoshikawa, 1990). Note, however, that the position of the origin is the same for both the virtual instrument system and the initial instrument system. Nevertheless, the frames differ in their orientations. Therefore, in a second step, we extract the corresponding rotation angles, which lead to this difference. To do this, we need to know the transformation from ${}^K_I T$ (initial position) to ${}^K_V T$ (desired position). In other words: we have to calculate ${}^I_V T$. This is done by taking the inverse matrix of the description of the initial position: ${}^K_I T^{-1} = {}^I_K T$. Now we get ${}^I_V T$ by matrix multiplication:

${}^I_V T = {}^I_K T \cdot {}^K_V T$. Based on this result, we can determine the X-Y-Z Yaw-Pitch-Roll rotation angles for the instrument as follows:

$$\alpha_V = atan2({}^I_V T_{21}, {}^I_V T_{22}) \quad (3)$$

$$\beta_V = atan2(-{}^I_V T_{20}, \sqrt{{}^I_V T^2_{00} + {}^I_V T^2_{10}}) \quad (4)$$

$$\gamma_V = atan2({}^I_V T_{10}, {}^I_V T_{00}) \quad (5)$$

We now have the rotation angles of the virtual instrument from its initial position to the desired pose. In the definition of V (see above) we assumed that all rotation axes of the virtual instrument intersect in one point.

We now have to consider how to simulate this behavior with the real instrument and its mechanical axes. The mechanical x_M-axis and the virtual x_V-axis are identical by definition. That means we can directly apply the x_V-rotation of the virtual instrument to its mechanical counterpart, the yaw of the fingers ($\alpha_M = \alpha_V$).

Because the x_M and y_M-axis of the instrument do not intersect, we cannot apply the y_V-rotation without modifications. We have to calculate it from known geometric properties of the set-up: (i) the rotation angle about the y_V-axis of the virtual instrument (β_V) is known, (ii) the shaft of the instrument always passes through the port P and (iii) though not necessarily identical, virtual and mechanical y-axis are always parallel. Using these properties we can compute the rotation about the mechanical y_M-axis (β_M). Note that the position of V remains unchanged but the shaft of the instrument is tilted about the port. As can

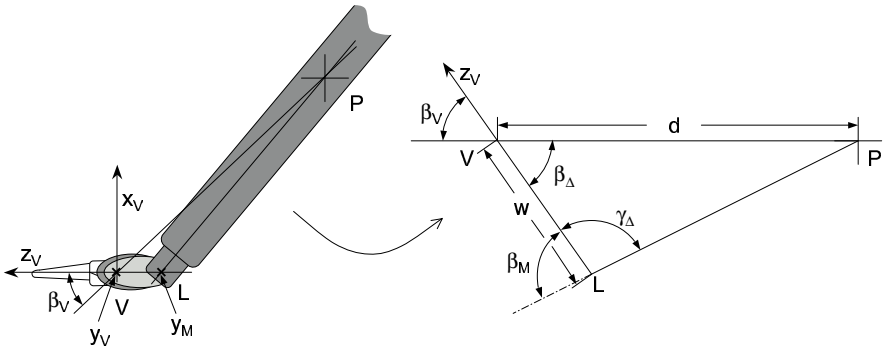

Figure 6. Determination of β_M

be seen in Fig. 6, two sides of a triangle are known, with w being the length of the instrument's wrist and d being the distance between the port and the position of the virtual instrument system. Additionally we

are given the rotation angle $\beta_\triangle = \beta_V$ which is constituted by w and d. Therefore the following holds:

$$\tan\left(\frac{\gamma_\triangle - \alpha_\triangle}{2}\right) = \frac{d-w}{d+w}\cot\left(\frac{\beta_\triangle}{2}\right) \quad (6)$$

$$\frac{\gamma_\triangle + \alpha_\triangle}{2} = 90^\circ - \frac{1}{2}\beta_\triangle; \quad (7)$$

By applying the atan-function to Eq. (6) and adding (7), we have:

$$\gamma_\triangle = \tan^{-1}\left(\frac{d-w}{d+w}\cot\left(\frac{\beta_\triangle}{2}\right)\right) + 90^\circ - \frac{1}{2}\beta_\triangle \quad (8)$$

Moreover, $\beta_M = 180^\circ - \gamma_\triangle$.

The last angle to determine is the mechanical rotation of the instrument's shaft. The initial transformation of the shaft is set by the transformation of the robot flange F. In order to reach the desired position of the virtual instrument, we perform a rotation about the z_I-axis (see derivation of transform ${}^I_V T$). On the other hand, we only can apply rotations about the real z_M-axis, which is identical with the z_F-axis (see Fig. 7). It is clear from picture 6 that the longitudinal axis of the shaft z_M ($\overrightarrow{PL}$) is not collinear with the z_I-axis ($\overrightarrow{PV}$) when β_M is not zero. In this case, we have to determine γ_M by an additional calculation. To this end we need to find the positions of the mechanical instrument axes (esp. the shaft axis $z_M = z_F$) relative to the robot base system. Our chosen convention for the y_F-axis is that it is initially parallel to the xy_K-plane. Note that every other convention would naturally change γ_M, but will not influence the final position of the instrument. In Fig. 7, the point V^+ is the position of the virtual instrument if γ_M were zero. We thus have to rotate the shaft until V^+ overlaps with the actual position of the virtual instrument $V = {}^K_V T_t$. In other words: we have to find the rotation transforming x_F, which is parallel to a plane spanned by z_K and $\overrightarrow{PL}$, to x_I, which is parallel to a plane spanned by $\overrightarrow{PL}$ and $\overrightarrow{PV}$ (see Fig. 7). Therefore we first have to find the position of the inflexion point L (also see Fig. 6). We know the transformation of the virtual instrument ${}^K_V T$. Since the x_V- and the x_M-axis are identical, we can get the orientation of the wrist ${}^K_W T_r$, by back-rotating ${}^K_V T$ by $-\alpha_M$. Because the z-axis of the resulting system points in the direction of the wrist, we can move back along it the known length of the wrist w. Thus, altogether we get:

$$\overrightarrow{L} = {}^K_V T \cdot {}^V_W T \cdot \begin{pmatrix} 0 \\ 0 \\ -w \\ 1 \end{pmatrix} \quad (9)$$

Given all the points, we can now estimate γ_M. The best way to do this is

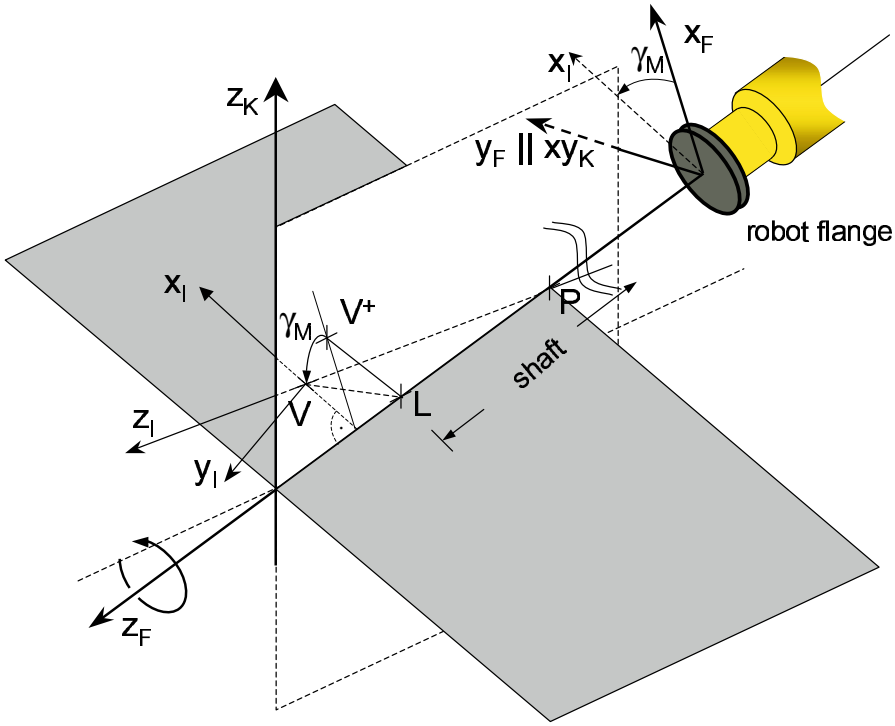

Figure 7. Calculation of γ_M

calculating the intersection angle of the plane spanned by V^+, L and P, and the plane spanned by V, L and P. We get this angle by intersecting the normals of these planes. Now we have all angles necessary to control the instrument.

The final step is to determine the position and rotation of the flange of the robot (${}^K_F T$), which the instrument attached to. Since we know the position of the port P and the inflexion point L (Fig. 6), we can determine the Z-Y-Z Euler-angles α_K, β_K and γ_K in a similar fashion we used for the rotation of the initial instrument (Fig. 5). Because we required parallelism of the y_i-axis of the initial virtual instrument system (cf. Fig. 4) with the xy_K-plane of the robot system, we set the rotation of the flange to zero. We have:

$$\alpha_K = atan2(P_y - L_y, P_x - L_x) \quad (10)$$

$$\beta_K = atan2(P_z - L_z, \sqrt{(P_x - L_x)^2 + (P_y - L_y)^2} + 90^\circ \quad (11)$$

$$\gamma_K = 0 \quad (12)$$

The position of the shaft can be found by shifting back L along $\overrightarrow{PL}$ for the length of the instrument. With orientation and position we can arrange the homogenous transform matrix of the flange. Given the transformation, we can derive the joint angles of the robot by standard inverse kinematics.

4. Simulation

In order to check certain operation sequences (e.g. the complicated procedure of knot-tying) before applying them to the real world, we have developed a realistic simulation of our system. Since the model has the same geometry as the real system, all joint angles obtained from the inverse kinematics can be directly applied to it. The model is displayed in an *Open Inventor*-GUI. Input data can be recorded to a data base for subsequent use with the simulation or the real system. This simulation was especially useful to detect some unusual motion sequences that could lead to failures of the real system. For example, the robot tends to move too fast if the instrument tips approach come too close to the port. The simulation can also be used in parallel with real manipulations. This can be very helpful if the remote user has no full sight of the operation environment (e.g. if instruments are occluded by other objects).

5. Conclusion

We have presented an experimental system for robot assisted minimally invasive surgery with haptic feedback. It enables full Cartesian control of the instruments by implementing trocar kinematics. This is an important aspect for increasing the acceptance of such systems with surgeons. We are currently working on further improvements of both, the real system and the simulation environment. The robotic system will be continued to be developed towards a reliable and stable surgical workstation. The future plans for the simulation environment include inclusion of haptic feedback by means of a realistic tissue model, thread modelling and implementation of augmented reality techniques.

References

Cavasoglu M. et al. (2003), Robotics for Telesurgery: Second Generation Berkeley/UCSF Laparoscopic Telesurgical Workstation and Looking towards the Future Applications, *Industrial Robot, Special Issues on Medical Robotics*, Vol. 30, no. 1

Craig, John J. (1986), Introduction to Robotics (Mechanics and Control), Addison Wesley, Massachusetts, USA.

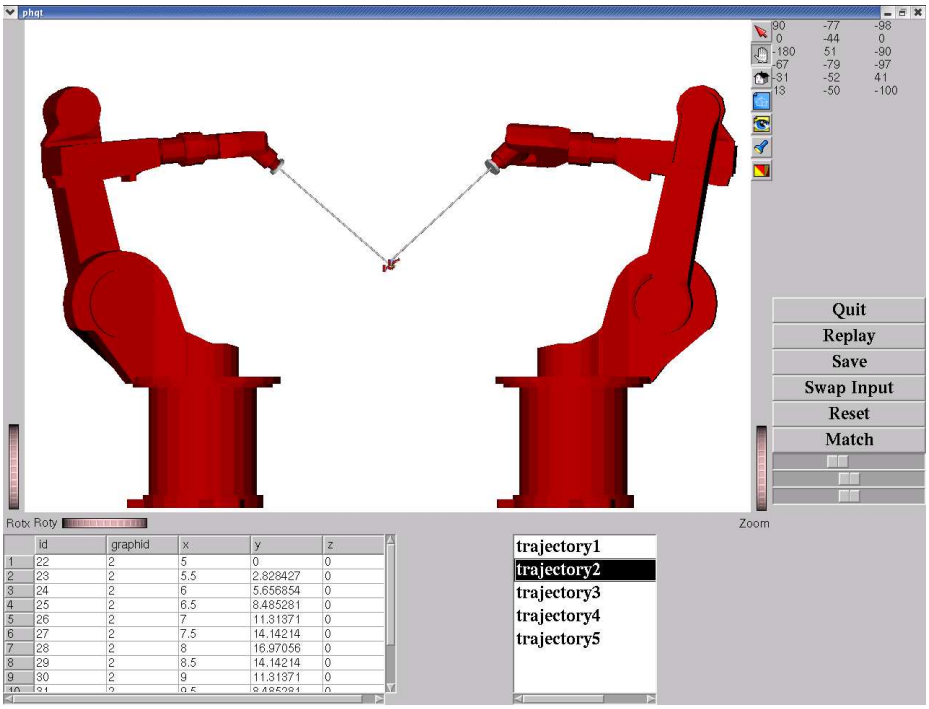

Figure 8. Screenshot of the Simulation Environment

Guthart, Gary S., and Salisbury, J. K. (2000), The Intuitive^{TM} Telesurgery System: Overview and Application, *IEEE International Conference on Robotics and Automation*, San Francisco CA, USA.

R. Konietschke et al. (2003), Optimal Design of a Medical Robot for Minimally Invasive Surgery, *2. Jahrestagung der Deutschen Gesellschaft fuer Computer- und Roboterassistierte Chirurgie (CURAC)*, Nuernberg, Germany

Kwon D. et al. (1998), Microsurgical Telerobot System, *IEEE/RSJ International Conference on Intelligent Robots and Systems*, pp. 945-950

Massie, Thomas. H. and Salisbury, J. Kenneth (1994), The PHANTOM Haptic Interface: A Device for Probing Virtual Objects, *Proceedings of the ASME Winter Annual Meeting, Symposium on Haptic Interfaces for Virtual Environment and Teleoperator Systems*, Chicago, IL, USA.

Voges U. et al., Evaluation of ARTEMIS: the Advanced Robotics and Telemanipulator System for Minimally Invasive Surgery, *Proceedings IARP 2nd Workshop on Medical Robotics*, pp. 137-148

Yoshikawa, Tsuneo (1990), Foundations of Robotics: Analysis and Control, MIT, Massachusetts, USA.